Chinese Chemical Letters 31 (2020) 1263–1266

Contents lists available at ScienceDirect

Chinese Chemical Letters

journal homepage: www.elsevier.com/locate/cclet

Communication

Hyperinoids A and B, two polycyclic meroterpenoids from *Hypericum patulum*

Xinyu Jia[a,c], Yongmei Wu[b], Chun Lei[a], Yanyan Yu[b], Jianqi Li[c,*], Jingya Li[b,*], Aijun Hou[a,*]

[a] School of Pharmacy, State Key Laboratory of Medical Neurobiology, Fudan University, Shanghai 201203, China
[b] National Center for Drug Screening, Shanghai Institute of Materia Medica, Chinese Academy of Sciences, Shanghai 201203, China
[c] Shanghai Institute of Pharmaceutical Industry, Shanghai 201203, China

ARTICLE INFO

Article history:
Received 21 August 2019
Received in revised form 13 October 2019
Accepted 14 October 2019
Available online 30 October 2019

Keywords:
Meroterpenoids
Hyperinoids A and B
Anti-inflammation
Hypericum patulum
Guttiferae

ABSTRACT

Hyperinoids A (**1**) and B (**2**), two prenylated acylphloroglucinol related meroterpenoids, were isolated from *Hypericum patulum*. Compound **1** incorporates an unprecedented 11,12-dioxatetracyclo [5.4.3.$0^{1,7}$.$0^{4,14}$]tetradecane system, while **2** possesses a unique 10,11-dioxatetracyclo[5.3.3.$0^{1,7}$.$0^{4,13}$] tridecane system. Their structures were established by spectroscopic analysis and X-ray crystallographic data. Compounds **1** and **2** were identified as potent NF-κB inhibitors and suppressed the LPS-induced inflammatory responses in RAW 246.7 macrophages and primary mouse BMDM cells

The genus *Hypericum* (Guttiferae) comprises about 460 species globally distributed in temperate and subtropical regions [1]. There are 64 species in China, and some of them have antibacterial, anti-inflammatory, and hemostatic efficacy [2]. The *Hypericum* plants have triggered interests of natural product chemists owing to an array of meroterpenoids they generated. These metabolites not only have diverse and complex structures derived from polyprenylated acylphloroglucinol core with prenyl, geranyl, and acyl groups, but also possess intriguing bioactivities including antidepressant, neuroprotective, anti-inflammatory, antitumor, antibacterial, and antiviral activities [3–6].

The plant *Hypericum patulum* is a shrub widespread in China and can be used as a folk medicine for the treatment of gonorrhea, hepatitis, cold, tonsillitis, and bruises [2]. Some novel prenylated acylphloroglucinol meroterpenoids from this plant have been reported previously [7–9]. As a continuing exploration to seek structurally diverse and biologically interesting meroterpenoids from higher plants [10–12], phytochemical investigation on the aerial parts of *H. patulum* afforded two novel tetracyclic meroterpenoids, hyperinoids A (**1**) and B (**2**) (Fig. 1). Both structures with absolute configurations were elucidated by extensive analysis of NMR, MS, and X-ray crystallographic data. Compounds **1** and **2** possess two unprecedented tetracyclic systems of 11,12-dioxatetracyclo[5.4.3.$0^{1,7}$.$0^{4,14}$]tetradecane and 10,11-dioxatetracyclo[5.3.3.$0^{1,7}$.$0^{4,13}$]tridecane, respectively.

Nuclear factor-κB (NF-κB) is a key regulator of inflammation, and activation of NF-κB promotes inflammation-associated metabolic disorders such as obesity, type 2 diabetes, and atherosclerosis [13]. Macrophages, as innate immune cells, have been recognized as essential effector cells in the initiation and development of inflammation and insulin resistance [14]. For the discovery of bioactive natural products against inflammation-associated metabolic diseases, compounds **1** and **2** were investigated for the inhibitory activities in NF-κB pathway luciferase assay and the effects on the LPS-induced inflammatory responses in macrophages. In this paper, the structural identification and bioactivity evaluation of **1** and **2** are discussed.

Hyperinoid A (**1**) was isolated as colorless crystals with a specific rotation of $[\alpha]_D^{25}$ +54.0. Its molecular formula was determined to be $C_{32}H_{42}O_6$ by the HR-MS (ESI-TOF) ion at *m/z* 523.3057 $[M+H]^+$ (calcd. for $C_{32}H_{43}O_6$: 523.3054), indicating 12 indices of hydrogen deficiency. The IR spectrum of **1** showed absorption bands for OH (3442 cm^{-1}), carbonyl (1780 and 1737 cm^{-1}), and aromatic (1654 and 1465 cm^{-1}) functionalities. The ^1H NMR spectrum displayed characteristic signals for a monosubstituted benzene ring (δ_H 7.88, H-18/H-22; δ_H 7.51, H-20; δ_H 7.42, H-19/H-21), two olefinic protons (δ_H 4.78, H-24; δ_H 5.12, H-29), and seven singlet methyls (δ_H 1.15, H_3-10; 1.09, H_3-14; 1.05, H_3-15; 1.34, H_3-26; 1.18, H_3-27; 1.73, H_3-31; 1.66, H_3-32) (Table 1).

* Corresponding authors.
E-mail addresses: lijianqb@126.com (J. Li), jyli@simm.ac.cn (J. Li), ajhou@shmu.edu.cn (A. Hou).

https://doi.org/10.1016/j.cclet.2019.10.014
1001-8417/

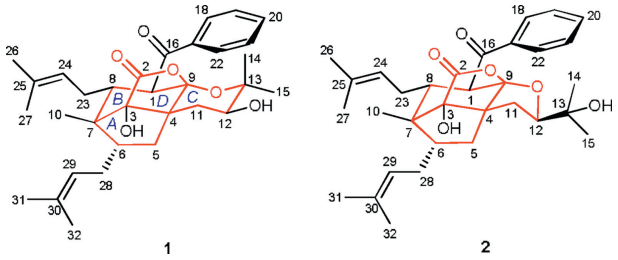

Fig. 1. Structures of hyperinoids A (**1**) and B (**2**).

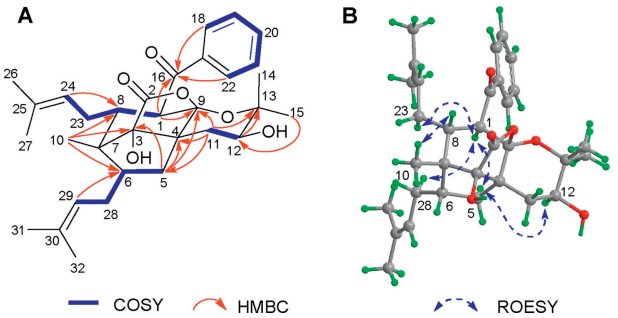

Fig. 2. Key 2D NMR correlations for **1**.

The ^{13}C NMR, DEPT, and HSQC spectra revealed 32 carbon resonances (Table 1), assignable to a benzoyl moiety, an ester carbonyl (δ_C 174.0, C-2), one ketal carbon (δ_H 109.1, C-9), two prenyl (3-methylbut-2-enyl) groups, three methyls, two methylenes, four methines (one oxygenated at δ_C 70.9, C-12), two oxygenated tertiary carbons (δ_C 91.2, C-3; δ_C 79.0, C-13), and two quaternary carbons. These data accounted for eight indices of hydrogen deficiency, and the remaining ones required the existence of four additional rings in **1**. Therefore, **1** was speculated to have a tetracyclic system decorated with a benzoyl and two prenyl groups.

The planar structure of **1** was established by extensive analysis of its ^1H-^1H COSY and HMBC spectra (Fig. 2A). The ^1H-^1H COSY correlations of H-1/H-8 and H-5/H-6 and the HMBC cross-peaks of H_3-10/C-3, C-6, C-8; H_2-5/C-3, C-4, C-9; and H-1/C-9 established a cyclopentane (ring A) and a cyclohexane (ring B). The ^1H-^1H COSY correlations of H-11/H-12 and the HMBC networks of H-11/C-4, C-5, C-9, C-13; H-12/C-13; and H_3-14, 15/C-12 defined a 3-hydroxy-2,2-dimethyltetrahydropyran ring (ring C). The remaining ring (ring D) was formed by a lactone bridge between C-3 and C-9, as suggested by the diagnostic chemical shifts of C-2, C-3, and C-9. Furthermore, the HMBC correlations of H-29/C-6 and H-24/C-8 and the ^1H-^1H COSY correlations of H-6/H_2-28/H-29 and H-8/H_2-23/H-24 showed that the two prenyl groups were connected to C-6 and C-8, respectively. The benzoyl group was connected to C-1, as revealed by the HMBC correlations of H-1/C-16 and H-18, H-22/C-16. Thus, the gross structure of **1** was deduced as a meroterpenoid with an unprecedented 11,12-dioxatetracyclo[5.4.3.$0^{1,7}$.$0^{4,14}$]tetradecane ring system.

The coupling constant of H-1/H-8 (J =11.4 Hz) and the H-1/H-23b ROESY cross-peak (Fig. 2B) indicated that H-1 and H-8 were axially *trans*-oriented, and they were then assigned an α-orientation and a β-orientation, respectively. The H_3-10/H-8 ROESY correlation suggested an equatorial β-orientation for H_3-10. The H-1/H-28b, H-1/H-5α, and H-5α/H-12 ROESY correlations revealed that the prenyl group at C-6 and H-12 were α-oriented. The relative configurations at C-3, C-4, and C-9 could not be elucidated by ROESY experiment. But owing to the restriction by the rigid tetradecane ring system, they could be assigned as 3*R**, 4*S**, and 9*R**. A single-crystal X-ray diffraction experiment for **1** was conducted by Ga Kα radiation with an absolute structure parameter of 0.04(6) (Fig. 3). Thus, the absolute configuration of **1** was established as 1*S*, 3*R*, 4*S*, 6*S*, 7*R*, 8*R*, 9*R*, and 12*S*.

Hyperinoid B (**2**) was obtained as colorless crystals and had optical activity ($[\alpha]_D^{25}$ +61.0). The molecular formula $C_{32}H_{42}O_6$ was established by the HR-MS (ESI-TOF) ion at m/z 523.3056 $[M+H]^+$

Table 1
^1H (600 MHz) and ^{13}C (150 MHz) NMR data of **1** and **2** in $CDCl_3$.

No.	**1**		**2**	
	δ_H, multi (J in Hz)	δ_C	δ_H, multi (J in Hz)	δ_C
1	3.83, d (11.4)	51.6	3.88, d (10.8)	49.9
2		174.0		173.1
3		91.2		91.3
4		57.5		64.1
5	β 2.01, dd (13.8, 10.2) α 1.87, dd (13.8, 9.6)	37.9	β 2.12, dd (14.4, 10.8) α 1.83[a]	36.9
6	2.40, m	49.1	2.46, m	48.3
7		52.3		53.9
8	2.27, m	45.6	2.33[a]	46.6
9		109.1		116.0
10	1.15, s	16.4	1.18, s	16.4
11	1.83, d (8.4)	31.3	β 2.33[a] α 1.83[a]	30.4
12	3.60, t (8.4)	70.9	4.32, dd (10.8, 6.0)	91.6
13		79.0		70.2
14	1.09, s	19.9	1.00, s	24.2
15	1.05, s	28.2	0.98, s	27.2
16		196.7		195.5
17		139.5		138.6
18	7.88, br d (7.2)	128.8	7.92, br d (7.2)	128.8
19	7.42, t (7.2)	128.1	7.45, t (7.2)	128.3
20	7.51, br t (7.2)	132.4	7.54, br t (7.2)	132.9
21	7.42, t (7.2)	128.1	7.45, t (7.2)	128.3
22	7.88, br d (7.2)	128.8	7.92, br d (7.2)	128.8
23	a 2.35, m b 1.95, dt (15.0, 7.2)	29.5	a 2.40[a] b 2.04, dt (15.0, 7.2)	29.5
24	4.78, t (7.2)	125.6	4.85, t (7.2)	125.6
25		131.9		132.0
26	1.34, s	25.6	1.36, s	25.6
27	1.18, s	17.5	1.24, s	17.6
28	a 2.37, m b 2.19, m	30.3	a 2.40[a] b 2.21, m	30.1
29	5.12, t (7.2)	123.4	5.12, t (6.6)	123.4
30		133.0		133.1
31	1.73, s	25.9	1.73, s	25.9
32	1.66, s	18.1	1.68, s	18.2

[a] The signals are overlapped.

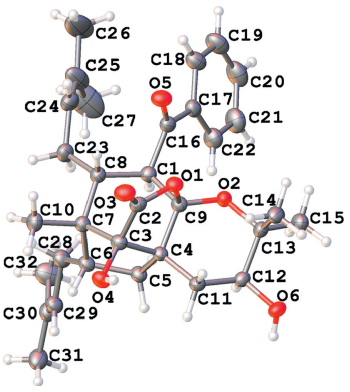

Fig. 3. Single-crystal X-ray plot for **1**.

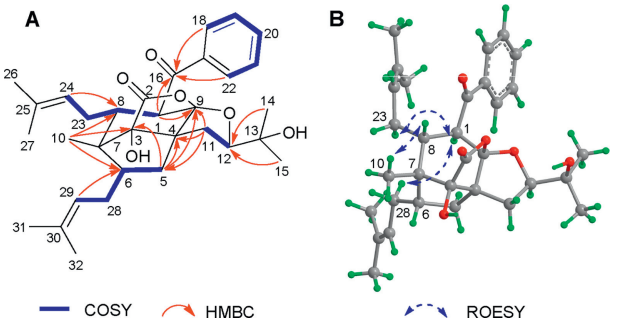

Fig. 4. Key 2D NMR correlations for **2**.

(calcd. for $C_{32}H_{43}O_6$: 523.3054). Interpretation of its NMR data (Table 1) including ^{1}H-^{1}H COSY and HMBC spectra (Fig. 4A) indicated that **2** was also a tetracyclic meroterpenoid with the same rings A, B, and D moieties as **1**. The only difference between them was the ring C. Compound **2** contained a 2-(1-hydroxy-1-methylethyl)tetrahydrofuran ring rather than the 3-hydroxy-2,2-dimethyltetrahydropyran moiety in **1**, as supported by the obviously downfield-shifted C-12 (δ_C 91.6), the oxygenated C-13 (δ_C 70.2), and the ^{1}H-^{1}H COSY and HMBC correlations shown in Fig. 4A.

The relative configurations at C-1, C-6, C-7, and C-8 were consistent with those of **1**, as verified by the coupling constant of H-1/H-8 (J =10.8 Hz) and the ROESY correlations of H-1/H-23b, H_3-10/H-8, and H-1/H-28b (Fig. 4B). Similar to **1**, the 3*R**, 4*S**, and 9*R** configurations were also deduced by the rigidity of the skeleton. The configuration at C-12 could not be defined from the available data. Fortunately, the absolute configuration of **2** was finally assigned as 1*S*, 3*R*, 4*S*, 6*S*, 7*R*, 8*R*, 9*R*, and 12*R* by an X-ray crystallographic study (Ga Kα radiation) with an absolute structure parameter of 0.02(9) (Fig. 5). Compound **2** is the first meroterpenoid possessing a novel 10,11-dioxatetracyclo[5.3.3.0^{1,7}.0^{4,13}]tridecane ring system.

Compounds **1** and **2** were proposed to biogenetically originate from the prenylated acylphloroglucinol precursor **i** (Scheme 1). It would undergo intramolecular cyclization to form **ii**, which after oxidative ring cleavage would give **iii**. Through decarboxylation, intermediate **iv** would be formed [7]. After epoxidation and intramolecular nucleophilic addition, the hemiketal intermediate **v** would be produced. Then, **1** and **2** would be formed *via* two different ring opening pathways of epoxide.

In order to discover natural products against inflammation-associated metabolic diseases, compounds **1** and **2** were evaluated for their anti-inflammatory effects *in vitro*. Compounds **1** and **2** exhibited significant inhibitory activities in NF-κB pathway luciferase assay with IC_{50} values of 0.75 ± 0.17 and

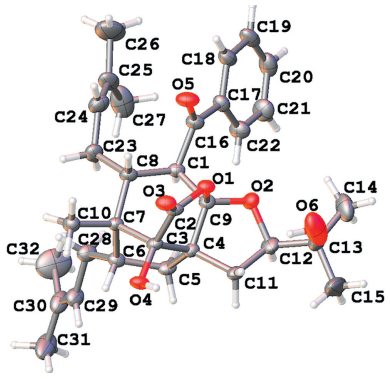

Fig. 5. Single-crystal X-ray plot for **2**.

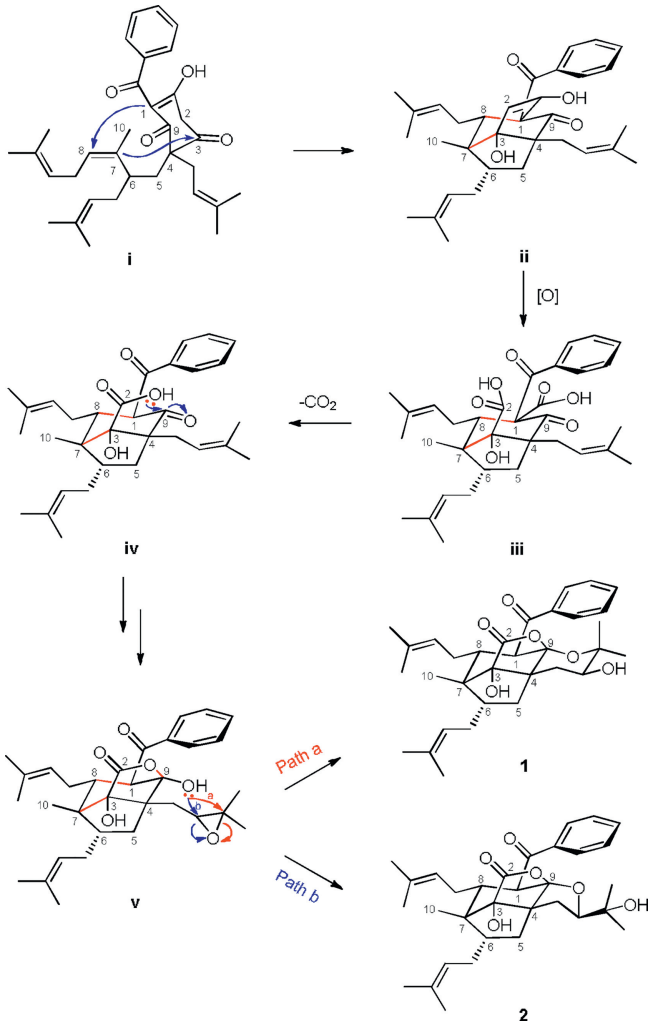

Scheme 1. Putative biosynthetic pathway for compounds **1** and **2**.

1.19 ± 0.48 μmol/L, respectively. In this test, bortezomib (PS-341) was used as the positive control ($IC_{50} = 0.07 \pm 0.01$ μmol/L). They were further evaluated for influences on the LPS-induced inflammatory responses in RAW 246.7 macrophages and primary mouse BMDM cells. The MTS assay showed no obvious cytotoxicity against RAW 246.7 cells at the tested concentrations (Fig. S1 in Supporting information). The mRNA levels of some pro-inflammatory genes, such as IL-1β, IL-6, and iNOS, were downregulated by **1** and **2** (Fig. 6).

In summary, hyperinoids A (**1**) and B (**2**), two meroterpenoids biogenetically related to prenylated acylphloroglucinols, were obtained from *H. patulum*. The majority of meroterpenoids from the genus *Hypericum* belong to the bicyclic polyprenylated acylphloroglucinols featuring a bicyclo[3.3.1]nonane-2,4,9-trione core, the adamantane-type with tricyclo[3.3.1.1]decane skeleton, and the homoadamantane-type with tricyclo[4.3.1.1]undecane motif [3]. Different from them, compounds **1** and **2** possess two unprecedented tetracyclic systems of 11,12-dioxatetracyclo[5.4.3.0^{1,7}.0^{4,14}]tetradecane and 10,11-dioxatetracyclo[5.3.3.0^{1,7}.04,^{13}]tridecane, respectively, derived from a rare bicyclo[3.2.1]octane framework [7]. Both of them showed significant anti-inflammatory effects *in vitro*. They are potent NF-κB pathway inhibitors and can effectively decrease the inflammatory response of macrophages. The novel structures and significant bioactivities of **1** and **2** may provide useful reference for discovering and designing drug leads against inflammation-related metabolic diseases.

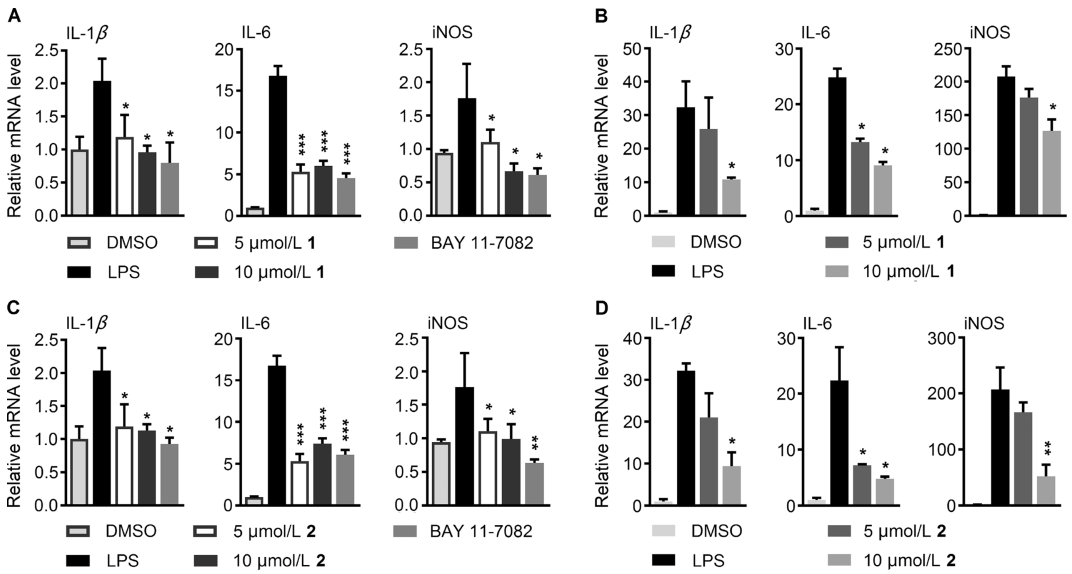

Fig. 6. Effects of compounds **1** and **2** on the LPS-induced inflammatory response in macrophages: Effects of **1** (A) and **2** (C) on the LPS-induced genes expression in RAW 246.7 cells. Effects of **1** (B) and **2** (D) on the LPS-induced genes expression in primary mouse BMDM cells. Cells were treated with LPS alone or together with **1** or **2** for 24 h. BAY 11-7082 (10 μmol/L) was used as the positive control. Results are given as mean ± SEM ($n = 3$). $^{*}P < 0.05$, $^{**}P < 0.01$, $^{***}P < 0.001$.

Declaration of competing interest

The authors declare that they have no known competing financial interests or personal relationships that could have appeared to influence the work reported in this paper.

Acknowledgment

This research was financially supported by Fudan-SIMM Joint Research Fund (No. FU-SIMM20181011).

Appendix A. Supplementary data

Supplementary material related to this article can be found, in the online version, at doi:https://doi.org/10.1016/j.cclet.2019.10.014.

References

[1] X. Li, N.K.B. Robson, Flora of China, Vol. 13, Science Press, Beijing, 2007, pp. 2–35.
[2] State Administration of Traditional Chinese Medicine of the People's Republic of China, Chinese Materia Medica, Vol. 9, Shanghai Scientific and Technical Publishers, Shanghai, 1999, pp. 594–608.
[3] X.W. Yang, R.B. Grossman, G. Xu, Chem. Rev. 118 (2018) 3508–3558.
[4] H. Bridi, G.C. Meirelles, G.L. von Poser, Phytochemistry 155 (2018) 203–232.
[5] Y.L. Hu, K. Hu, L.M. Kong, et al., Org. Lett. 21 (2019) 1007–1010.
[6] X.T. Yan, Z. An, Y. Huangfu, et al., Phytochemistry 159 (2019) 65–74.
[7] N. Tanaka, Y. Yano, Y. Tatano, et al., Org. Lett. 18 (2016) 5360–5363.
[8] Y.Y. Liu, Z. Ao, G.M. Xue, et al., Org. Lett. 20 (2018) 7953–7956.
[9] Z.N. Wu, Q.W. Niu, Y.B. Zhang, et al., RSC Adv. 9 (2019) 7961–7966.
[10] H.B. Liao, C. Lei, L.X. Gao, et al., Org. Lett. 17 (2015) 5040–5043.
[11] H.B. Liao, G.H. Huang, M.H. Yu, et al., J. Org. Chem. 82 (2017) 1632–1637.
[12] G.H. Huang, Z. Hu, C. Lei, et al., J. Nat. Prod. 81 (2018) 1810–1818.
[13] R.G. Baker, M.S. Hayden, S. Ghosh, Cell Metab. 13 (2011) 11–22..
[14] J.C. McNelis, J.M. Olefsky, Immunity 41 (2014) 36–48.